Photon spectrum associated with radiative electron-capture processes

J. E. Miraglia, C. R. Garibotti,* and A. D. González
Instituto de Astronomía y Física del Espacio, Consejo Nacional de Investigaciones Científicas y Técnicas, Casilla de Correos 67, Sucursal 28, 1428 Capital Federal (Buenos Aires), Argentina
(Received 8 November 1984)

Three-body calculations of photon spectra associated with radiative electron capture are carried out by using the first-order Born approximation. Shell-to-shell results are presented. The theory is compared with experimental results measured at 90° to the incident beam. Structures occurring in the experiments are explained in terms of transitions to higher shells of the projectile coming from K or higher shells of the target.

I. INTRODUCTION

Radiative electron capture (REC) by fast ions was first identified by Schnopper *et al.*[1] One year later, Kienle *et al.*[2] (hereinafter referred to as I) measured x-ray cross sections, at 90° to the incident beam, when high-energy Ar^{17+} and Ne^{10+} ions passed through He and Ne neutral targets. Later on, some other REC experiments were reported by using solid[3,4] and gas targets.[5]

As a first theoretical approach, the REC can be considered as a binary electron-projectile (e-P) radiative recombination process,[6] which is fully independent of the target nucleus (T). In the simplest version the electron is considered "at rest" in the target. The process is seen, from the projectile frame, as a radiative transition from the continuum state, with relative velocity v, to a bound state with energy ϵ_f. Then, it follows that the photon spectrum profile is a δ Dirac function placed at $v^2/2-\epsilon_f$, which can be integrated to obtain the total cross section[7] (atomic units are used, unless otherwise stated).

The e-P binary model can be substantially improved if the active electron is described by a wave packet given by the momentum distribution of the initial electronic state.[2-5] In this case the photon spectrum is no longer the δ Dirac function but the so-called Compton profile. Calculations have been carried out in I using this description and neglecting the P-e continuum interaction. In this model, Kienle *et al.*[2] found that contributions from projectile electronic states, other than the ground state, were very small (in contrast, as we shall see, to the conclusion of the present work). The theoretical model used in I proved to be, in general, reliable. However, when compared with the experiments, two disagreements were found, viz, the following:

(a) The high-energy x-ray tail was much higher than the theoretical results provided by such an improved binary model.

(b) Other enhancements or structures in the photon spectrum could not be explained.

To explain the first disagreement, Kienle *et al.*[2] proposed a new process of photon emission which was ascribed to the bremsstrahlung from initially bound electrons of the target in the Coulomb field of the projectile. The photon yield in this new mechanism—which could be called radiative ionization—was evaluated and multiplied by a factor depending on the system. When the photon spectrum associated with this new process is added to the REC one, then good agreement with the experiments is found for the high-energy x-ray tail (see dashed line in Fig. 2). However, the second disagreement was not explained. The aim of the present work is to prove that such structures occurring in the experimental photon spectrum can be attributed to transitions to higher shells of the projectile.

So far, we have summarized the main records of the binary model. This approach has achieved a moderate degree of agreement with the experiments at high projectile energies. In the present work we have carried out *three-particle* calculations, which let the nuclei be active particles during the collision. This approach is certainly more appropriate, particularly in the intermediate region of the incident projectile energy. Since the exact three-particle wave function is unknown, the results will depend on the approximation used.

The first three-particle formulation of the REC was worked out by Briggs and Dettmann[8,9] in the impact-parameter method. After several peaking approximations, they have shown that the high-energy limit of the REC total cross section, calculated with the first-order Born approximation, coincides with the binary model. The strong-potential Born approximation, which is a three-particle theory, has been examined by Gorriz *et al.*[10] They have found that off-shell states, included in this approximation, can lead to significant contribution to the differential and total REC cross sections, even at high projectile velocities. More recently, we have calculated total and differential REC cross sections[11] by using the continuum distorted-wave theoretical method.[12] It was verified that the radiative—and not the mechanical—is the dominant electron-capture mechanism at very high, but not relativistic, projectile energies.

II. THEORY

In the present work we have followed the theoretical treatment outlined by Briggs and Dettmann.[8,9] The theory can be summarized as follows. The total Hamil-

tonian is $H=H_m+H_r$, where H_m is the three-particle mechanical Hamiltonian and H_r is the radiation-matter interaction given by

$$H_r=i\left[\frac{2\pi}{\omega}\right]^{1/2}\hat{\lambda}_j\cdot\nabla_{\mathbf{r}_p}\ , \tag{1}$$

where $\hat{\lambda}_j$ is the polarization vector, ω is the photon energy, and $\mathbf{r}_P$ is the P-e coordinate. In first perturbative order the matrix element of H_r is[8–12]

$$\langle H_r\rangle_{fi}=\langle\Psi_f^-\,|\,H_r\,|\,\Psi_i^+\rangle\ , \tag{2}$$

where Ψ_f^- and Ψ_i^+ are the *exact* solutions of H_m. Using first-order-Born wave functions for the three-particle system (P, T, and e), it reads

$$\langle H_r\rangle_{fi}^{\text{Born}}=i\left[\frac{2\pi}{\omega}\right]^{1/2}\hat{\lambda}_j\int\int e^{-i\mathbf{K}_f\cdot\mathbf{R}_P}\phi_f^*(\mathbf{r}_P)\times\nabla_{\mathbf{r}_p}e^{i\mathbf{K}_i\cdot\mathbf{R}_T}\phi_i(\mathbf{r}_T)$$

$$=\left[\frac{2\pi}{\omega}\right]^{1/2}\tilde{\phi}_i(\mathbf{W}_T)\tilde{\phi}_f^*(\mathbf{W}_P)\hat{\lambda}_j\mathbf{W}_P\ , \tag{3}$$

where $\{\mathbf{R}_T,\mathbf{r}_T\}$ and $\{\mathbf{R}_P,\mathbf{r}_P\}$ represent the usual reactive coordinate systems (see, for example, Ref. 10), and ϕ_i and ϕ_f are the initial and final quantum states of the electron. The tildes stand for the Fourier transforms, $\mathbf{K}_i$ is the initial momentum of the projectile, and $\mathbf{K}_f$ is the final momentum of the rearranged atom. Also in Eq. (3)

$$\mathbf{W}_T=\mathbf{K}_f-\mu_T\mathbf{K}_i,\quad \mathbf{W}_P=\mathbf{v}-\mathbf{W}_P=\mathbf{K}_i-\mu_P\mathbf{K}_f\ , \tag{4}$$

where μ_T and μ_P are the T-e and P-e reduced masses.

The fivefold differential cross section reads[10,11]

$$\frac{d^{(5)}\sigma_{\text{Born}}^{\text{REC}}}{d\omega\,d\Omega\,d\Omega'}=\frac{\omega\nu_T\nu_P}{2^4\pi^4c^3}\,|\,\tilde{\phi}_i(\mathbf{W}_T)\tilde{\phi}_f^*(\mathbf{W}_P)\,|^2\sum_{j=1}^{2}|\,\hat{\lambda}_j\cdot\mathbf{W}_P\,|^2\ , \tag{5}$$

where $d\Omega$ and $d\Omega'$ are the differential solid angle of the photon and projectile, respectively, ν_T and ν_P are the P-$(T+e)$ and T-$(P+e)$ reduced masses, and c is the light velocity. To obtain the triple differential cross section on the photon energy space, an integration on the final-atom angular distribution is needed, i.e.,

$$\frac{d^{(3)}\sigma_{\text{Born}}^{\text{REC}}}{d\omega\,d\Omega}=\int d\Omega'\left[\frac{d^{(5)}\sigma_{\text{Born}}^{\text{REC}}}{d\omega\,d\Omega\,d\Omega'}\right] \tag{6}$$

which was numerically carried out. Clementi-Roetti wave functions were used to describe the electronic initial state,[13] and the result was multiplied by 2 to take into account the pasive electron. The Fourier transforms required in Eq. (5) were performed with the closed forms of Flannery.[14]

The x-ray spectrum associated with the REC for the $i\to f$ transition is found to be an enhancement with a shape determined by the momentum distribution of the initial state $\tilde{\phi}_i(\mathbf{W}_T)$. The position of the peak occurs when W_T is minimum. Since the projectile is mainly scattered in the forward direction,[11] we only need to know the projection of $\mathbf{W}_T$ on the beam direction, that is,

$$\hat{\mathbf{v}}\cdot\mathbf{W}_T=\frac{v}{2}-\frac{\omega+\epsilon_i-\epsilon_f}{v}\ . \tag{7}$$

Setting this to zero, the position of the peak is then estimated to be at $\omega_0=v^2/2+\epsilon_i-\epsilon_f$. The width of the peak can be found to be of the order of $v\sqrt{|\epsilon_i|}$.

It is interesting to point out that the present theory also predicts another peak shaped by the Fourier transform of the final electronic state $\tilde{\phi}_f(\mathbf{W}_P)$. It occurs now when W_P is minimum, that is, at $\omega_1=\epsilon_f-\epsilon_i-v^2/2$. As the projectile velocity increases this peak escapes to the negative range of the photon energy, and so it cannot be seen in the emission range.

III. RESULTS

We compare the theoretical results with the experimental cross sections of photon emission measured at 90° to the incident beam.[2] Three systems have been considered, and the calculations are shown in Figs. 1–3. In Figs. 1(a)–3(a), we show shell-to-shell theoretical results, and in Figs. 1(b)–(3(b) these values were shifted and normalized to the experiments.

In Fig. 1 the results for the system

$$^{20}_{10}\text{Ne}^{10+}+{}_2\text{He}(1s^2)\to{}^{20}_{10}\text{Ne}^{9+}(n_fl_fm_f)+{}_2\text{He}^{+}(1s) \tag{8}$$

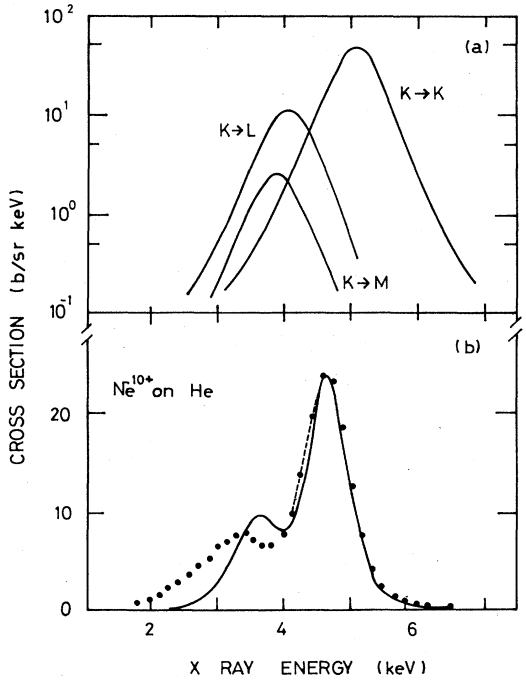

FIG. 1. Differential cross sections for x rays at 90° to the incident beam associated with the radiative electron capture process ${}_{10}\text{Ne}^{10+}+{}_2\text{He}\to{}_{10}\text{Ne}^{9+}+{}_2\text{He}^{+}$ at 7-MeV/amu incident energy. ——, present theoretical results; — — —, previous theoretical results from Kienle *et al.* (Ref. 2); ●, experimental results from Kienle *et al.* (Ref. 2) In (a) shell-to-shell theoretical results are displayed, in (b) they were summed and normalized to the experiments.

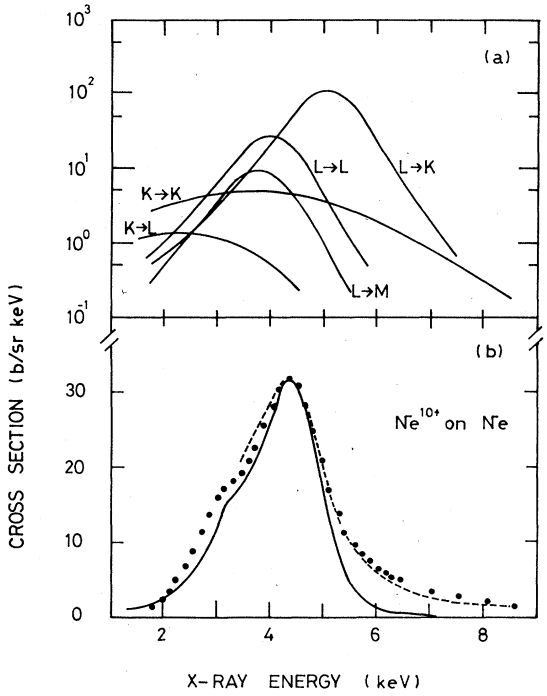

FIG. 2. Similar to Fig. 1 for the process $_{10}Ne^{10+}+{}_{10}Ne\rightarrow{}_{10}Ne^{9+}+{}_{30}Ne^{+}$ at 7-MeV/amu incident energy.

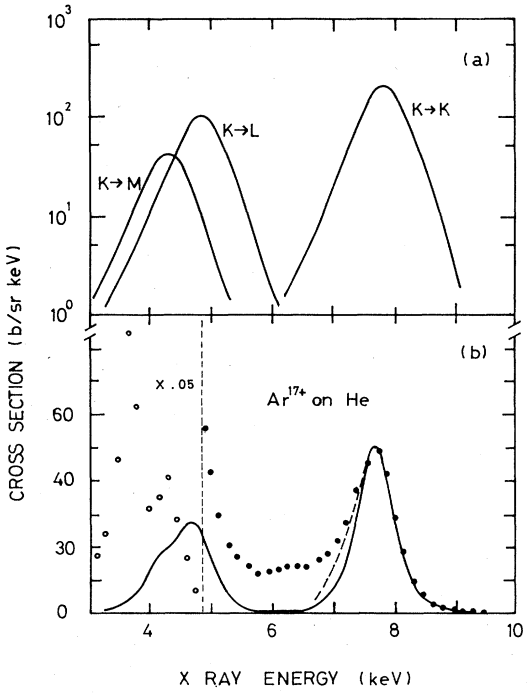

FIG. 3. Similar to Fig. 1 for the process $_{18}Ar^{17+}+{}_{2}He\rightarrow{}_{18}At^{16+}+{}_{2}He^{+}$ at 7.2-MeV/amu incident energy. Note: the empty circles represent the experiments multiplied by 0.05.

are displayed at 140-Mev incident energy. $K\rightarrow K$ ($1s\rightarrow 1s$), $K\rightarrow L$ ($1s\rightarrow 2s$, $1s\rightarrow 2p_{0,\pm 1}$), and $K\rightarrow M$ ($1s\rightarrow 3s$, $1s\rightarrow 3p_{0,\pm 1}$, $1s\rightarrow 3d_{0,\pm 1,\pm 2}$) transitions were considered. The normalization factor was 0.5. This value seems to fit with the following explanation: as known, the first-order Born approximation—used in this work—is valid at very high projectile energies. In the present case the ion velocity is 16.7, so it cannot be considered as very large if it is compared with the electron average velocity on the Ne K shell. In order to estimate, very roughly, the failure of the first order we resort to the e-P binary recombination model. In this process the ratio between the exact calculation (where the e-P continuum states is assumed) and the first-order Born approximation, for capturing to the ground state, is given by[4]

$$f(a)=\frac{2\pi a(1+a^2)}{1-\exp(-2\pi a)}\exp[-4a\tan^{-1}(1/a)]\ , \qquad (9)$$

where $a=Z/v$. For the Ne-He case we have $a=10/16.7=0.6$ and $f(0.6)=0.45$, which is very near to the 0.5 used here. Good agreement with the experiments is obtained for the $K\rightarrow K$ peak. The lower energy peak is now undoubtedly identified as capture to higher shells of the projectile.

In Fig. 2, we show the results for

$$^{20}_{10}Ne^{10+}+{}_{10}Ne(n_il_im_i)\rightarrow{}^{20}_{10}Ne^{9+}(n_fl_fm_f)+{}_{10}Ne^{+} \qquad (10)$$

at 140 Mev. Besides the $K\rightarrow K,L,M$ transitions, $L\rightarrow K,L,M$ ones also had to be calculated. The calculation for this system took around ten hours on our PDP 11/44 minicomputer. The theory gives a good account of the experiments near the maximum which comes from the $L\rightarrow K$ transition. This shows the relevance of including transitions from high shells of the target. The $L\rightarrow K$ transition is the dominant one because the L-shell electrons of the target are less bound than the K-shell ones. We have to recall that here—unlike on the mechanical electron capture—all the electron on the target, no matter the shell, give the same contribution to the total cross section at very high ion velocity. Another point of interest is that the present theory can explain the "shoulder" that occurs at 3.2 keV, which can be ascribed to $L\rightarrow L$ and $L\rightarrow M$ transitions. Here the $L\rightarrow M$ contribution is small but not negligible. The REC theory cannot account for the high-energy tail, since this has to be explained in terms of bremsstrahlung of strongly bound electrons, as described in I.

In Fig. 3 we display results for the process

$$^{40}_{18}Ar^{17+}+{}_{2}He(1s^2)\rightarrow{}^{40}_{18}Ar^{16+}(n_fl_fm_f)+{}_{2}He^{+}(1s) \qquad (11)$$

at 288 MeV. The argon ion was considered as a punctual particle with charge 17. As shown in the Fig. $K\rightarrow L,M$ transitions present an enhancement separated from the $K\rightarrow K$ one, with a similar yield. Unfortunately, for this particular system, the lower-energy peak cannot be identified from the experiments, since it is covered by radiative decay in the Ar ion [lines $K\alpha$ and $K\beta$ (Ref. 2)]. The normalization factor, in that case, is 0.24. Resorting to Eq. (9), we have $a=1$ and $f(1)=0.53$, which is larger than

the factor used. We can give an explanation to this disagreement as follows: as pointed out in I, the charge 17 was an average state, and it means that lower charges could occur in the beam. The projectiles with charges lower or equal to 16 have their K shell saturated, and then only $K \rightarrow L,M$ transitions can take place. This experimental situation could reduce the height of the $K \rightarrow K$ peak, and it also gives more relative importance to the lower energy peak. To proceed further, we would need to know the detailed state of charge of the incident beam. A final point to note is that here the ion velocity is equal to the average electron velocity on the argon K shell, and therefore the validity of a first-order calculation is doubtful.

In conclusion, we have shown that other enhancements can occur in the photon spectrum associated with REC processes. These new enhancements—not explained before—are due to the radiative electron capture into excited states of the projectile or capture of electrons coming from higher shells of the tangent.

---

*Instituto Balseiro, Comisión Nacional de Energía Atómica and Universidad Nacional de Cuyo, 8400 Bariloche, Argentina.

[1]H. W. Schnopper, D. H. Betz, J. P. Delvaille, K. Kalata, A. R. Sochval, K. W. Jones, and H. E. Wegner, Phys. Rev. Lett. **29**, 898 (1972).

[2]P. Kienle, M. Kleber, B. Povh, R. M. Diamond, F. S. Stephens, E. Grosse, M. R. Maier, and D. Proetel, Phys. Rev. Lett. **31**, 1099 (1973).

[3]E. Spindler, H. D. Betz, and F. Bell, J. Phys. B **15**, L561 (1977).

[4]R. Anholt, S. A. Andramonje, E. Morenzoni, Ch. Stoller, J. D. Molitoris, W. E. Meyerhof, H. Bowman, J. S. Xu, Z. Z. Xu, J. O. Rasmussen, and D. H. H. Hoffman, Phys. Rev. Lett. **53**, 234 (1984).

[5]H. Tawara, Patrick Richard, and K. Kawatsura, Phys. Rev. A **26**, 154 (1982).

[6]For discussions on two-particle recombination, see H. A. Bethe and E. E. Salpeter, *Quantum Mechanics of One- and Two-Electron Atoms* (Academic, New York, 1957). For radiative recombination into excited states, see A. Burgess, Mem. R. Astron. Soc. **69**, pt. 1 (1964).

[7]G. Raisbeck and F. Yiou, Phys. Rev. A **4**, 1858 (1971).

[8]J. S. Briggs and K. Dettmann, Phys. Rev. Lett. **33**, 1123 (1974).

[9]J. S. Briggs and K. Dettmann, J. Phys. B **10**, 1113 (1977).

[10]M. Gorriz, J. S. Briggs, and S. Alston, J. Phys. B **16**, L665 (1983).

[11]A. D. González and J. E. Miraglia, Phys. Rev. A **30**, 2292 (1984).

[12]I. M. Cheshire, Prov. Phys. Soc. London **84**, 89 (1964).

[13]E. Clementi and C. Roetti, At. Data Nucl. Data Tables **14**, 177 (1974), Table I.

[14]M. R. Flannery, Phys. Rev. **183**, 231 (1969).

[15]The normalization factor accounts for the failure of the Born approximation, as explained in the text; however, we have found no satisfactory explanation for the shifts. The resulting shifts were similar to those found in Ref. 2.